CHINESE OPTICS LETTERS

Vol. 22, No. 4 | April 2024

5 kW-level single-mode fiber amplifier based on low-numerical-aperture fiber

Yisha Chen (陈益沙)[1,2,3,†], Yun Ye (叶 云)[1,2,3,†], Liangjin Huang (黄良金)[1,2,3*], Huan Yang (杨 欢)[1,2,3], Hanshuo Wu (吴函烁)[1,2,3], Zhiping Yan (闫志平)[1,2,3], Zhiyong Pan (潘志勇)[1,2,3], Xiaolin Wang (王小林)[1,2,3**], Zefeng Wang (王泽锋)[1,2,3], and Pu Zhou (周 朴)[1]

[1] College of Advanced Interdisciplinary Studies, National University of Defense Technology, Changsha 410073, China

[2] Nanhu Laser Laboratory, National University of Defense Technology, Changsha 410073, China

[3] Hunan Provincial Key Laboratory of High Energy Laser Technology, National University of Defense Technology, Changsha 410073, China

[†]These authors contributed equally to this work.

*Corresponding author: hlj203@nudt.edu.cn

**Corresponding author: chinawxllin@163.com

Received November 13, 2023 | Accepted December 15, 2023 | Posted Online April 18, 2024

A low-numerical-aperture (NA) concept enables large-mode-area fiber with better single-mode operation ability, which is beneficial for transverse mode instability and nonlinear effects suppression. In this contribution, we reported a high-power fiber amplifier based on a piece of self-developed large-mode-area low-NA fiber with a core NA of 0.049 and a core/inner cladding diameter of 25/400 μm. The influence of the pump wavelength and fiber length on the power scaling potential of the fiber amplifier is systematically investigated. As a result, an output of 4.80 kW and a beam quality factor of ∼1.33 were finally obtained, which is the highest output power ever reported in a fiber amplifier exploiting the low-NA fiber. The results reveal that low-NA fibers have superiority in power scaling and beam quality maintenance at high power levels.

Keywords: high power fiber lasers; ytterbium-doped fiber; low-numerical-aperture fiber; mode instability.
DOI: 10.3788/COL202422.041404

1. Introduction

Due to the mature development of large-mode-area (LMA) fiber fabrication and the emergence of high-power, high-brightness pump sources and fiber-based functional components, the output power of high-power fiber laser (HPFL) has grown rapidly in the past two decades[1–4]. At present, the power scaling of HPFL is mainly limited by nonlinear effects such as stimulated Raman scattering (SRS) and stimulated Brillouin scattering (SBS). In order to suppress these nonlinear effects, LMA fiber is preferred and widely used in HPFL systems. However, as the core diameter increases, the number of propagation modes supported in the fiber core will inevitably increase, which may lead to direct deterioration of the output beam quality because of the amplification of the higher-order mode (HOM) contents. When the output power exceeds a certain threshold, the fluctuating energy transfer between the fundamental mode (FM) and the HOMs occurs, resulting in the sharp degeneration of the beam quality, which is now known as the onset of transverse mode instability (TMI). It is found that LMA fiber has a certain contradiction between large-mode field and single-mode operation. To alleviate or even eliminate this contradiction, reducing the fiber core NA is an effective method because highly differential bending loss between the FM and HOMs as well as a large-mode area can be achieved at the same time. In addition, since a low NA normally requires less rare-earth doping concentration, low-NA fibers also have the tendency in low photodarkening effect[5,6], which is potentially beneficial for long-term stability and TMI suppression[7,8]. Moreover, a decrease of fiber core NA will result in LP_{11} penetrating deeper into the fiber, and overlap between the LP_{11} mode and dopant area decrease is larger than the LP_{01} mode, like the mechanism of confined doping; thus the TMI threshold is increased[9]. However, pursuing an extremely too low NA will lead to weak confinement on the signal laser, which may cause a high loss of the dominant FM and a low slope efficiency. Furthermore, doping concentration is limited by the targeted low NA, leading to an increased requirement on the length of active fiber for efficient pump absorption, which, however, is detrimental to nonlinear effects suppression. Therefore, the fabrication process should be carefully designed to balance the pros and cons of the low NA to promote the single-mode power.

Considering the standard fabrication process of rare earth doped fiber by the modified chemical vapor deposition (MCVD) technique and the current industrial standard, we

define the fiber with the core NA less than 0.06 as the low-NA fiber[10]. In fact, the first demonstration of high-power application of the low-NA fiber can be dated to almost 20 years ago. Jeong *et al.* first-ever scaled the power of the single-mode fiber laser to kilowatts in 2004, and the core NA of the active fiber was below 0.05[11]. In 2014, Khitrov *et al.* fabricated a piece of ytterbium-doped fiber (YDF) with a core NA of 0.048, which supports the power scaling of the single-mode laser to 3 kW[12]. In 2015, Jain *et al.* successfully lowered the core NA to as low as 0.038[13], but the power of the all-fiber single-mode laser by using the fiber is only 585 W, limited by the onset of the TMI effects. The low TMI threshold can be attributed to the large guided modes number because of the relatively large core diameter (35 μm)[14]. In order to improve the TMI threshold, Beier *et al.* slightly increased the core NA to over 0.04 and decreased the core diameter to 24.5 μm, and achieved the output power of 3.0 kW limited by available pump power[15]. Subsequently, they achieved 4.3 kW single-mode output without tight bending and then achieved 4.4 kW by optimizing the fiber parameters and bending diameter, which is the highest single-mode fiber laser based on the low-NA fiber[16,17] before this contribution. The facts above fully demonstrate that low-NA fibers are capable of acquiring high power and high beam quality laser output.

However, a large proportion of publicly reported results with more than 1 kW output power are realized by employing all free-space format except Ref. [18]. Such high-power systems are not only required to be compact and stable, but care must be taken to avoid dusts and moisture. Furthermore, free-space fiber laser architectures have separated optical components and are vulnerable to mechanical vibration. In fact, an all-fiberized laser scheme can get rid of all the disadvantages of the free-space architecture through the fiber fusion splice process and avoidance of free-space optical components[18–20], which is preferable for practical applications.

In this work, we have fabricated a low-NA fiber and systematically studied the impact of pump wavelength on the power scalability of the all-fiberized low-NA fiber amplifier. By carefully designing the fiber with a slightly elevated core NA of ∼0.049, experimental results reveal that such a fiber is capable of realizing quasi-single-mode operation. By combining fiber design, pump wavelength shift (to 981 nm) from the dominant absorption peak (976 nm) and fiber length optimization, a 4.8 kW single-mode all-fiberized amplifier based on low-NA fiber is achieved. To the best of our knowledge, this report is the highest output power based on low-NA fiber ever reported so far. Moreover, discussions have been proposed for further optimization of fiber design and power scaling.

2. Experimental Setup

The low-NA double-clad YDF used in the experiment was prepared by the traditional MCVD process combined with gas phase doping technology. Compared with solution doping, gas phase doping can facilitate a more uniform Yb^{3+} distribution in radial and longitudinal directions and a more precise refractive index profile control with better repeatability[21,22]. The fiber has a core/inner cladding diameter of 25/400 μm, with a core NA of ∼0.049 and a cladding NA of ∼0.46. Noteworthily, this core NA is relatively close to conventional fiber NA of ∼0.06, and the fabrication process is more mature and can be better matched with conventional optical fiber devices. The refractive index profile of the as-fabricated fiber is depicted in Fig. 1(a). The absorption coefficient is measured to be ∼1.3 dB/m at 976 nm and ∼0.3 dB/m at 915 nm and shown in Fig. 1(b). According to the bending loss analytical formula, previously published by Marcuse[23], FM and HOM losses for NA = 0.049 at different bending radii are depicted in Fig. 1(c).

The as-fabricated low-NA fiber is then applied in a master oscillator power amplifier (MOPA) system for performance characterization. The system is based on an all-fiberized structure that consists of a low-power oscillator as the seed laser and a high-power main fiber amplifier. The seed laser employs YDF with the core/inner cladding diameter of 20/400 μm. The central wavelength of the seed laser is 1080 nm, the maximum output power is ∼100 W, and the corresponding beam quality factor M^2 is about $M_x^2 = 1.25$, $M_y^2 = 1.35$. The seed laser beam quality, spectrum, time domain, and corresponding FFT of the time domain are depicted in Fig. 2.

The main amplifier adopts a bidirectional pump scheme; the system schematic setup is shown in Fig. 3. The forward and backward pump power are injected into the fiber amplifier through forward and backward $(6 + 1) \times 1$ pump and signal combiners. The core/inner cladding diameters of the input and output signal fiber of both combiners are 25/250 μm and 25/400 μm, respectively, with a fiber core NA of about ∼0.06, and all pump ports of the combiners employ passive fiber with core/inner cladding diameter of 220/242 μm. A cladding light stripper (CLS) is spliced after the backward pump combiner

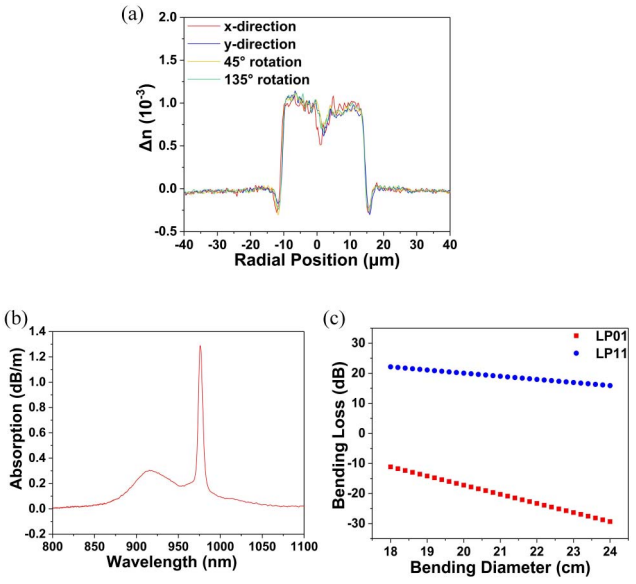

Fig. 1. (a) Refractive index profile. (b) Absorption coefficient. (c) Bending loss of FM and HOM at given bending diameter of low-NA fiber used in the experiment.

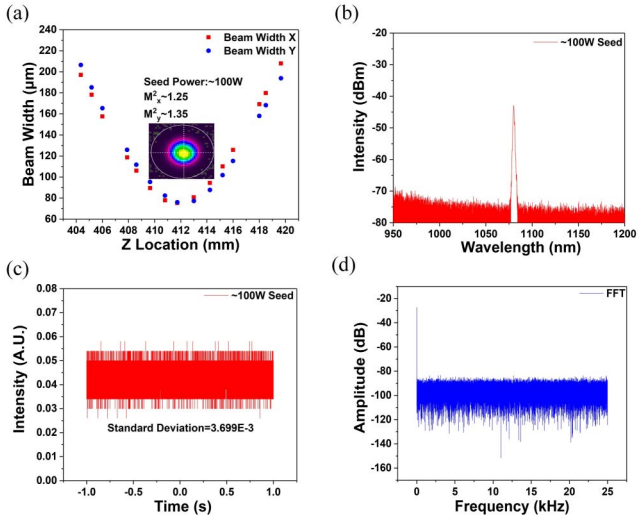

Fig. 2. (a) Beam quality; (b) spectrum; (c) time domain; (d) frequency domain of seed laser at output power of 100 W.

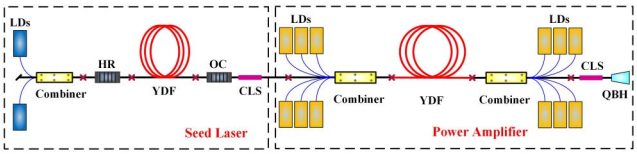

Fig. 3. Schematic setup of high-power low-NA fiber amplifier. LD, laser diode; HR, high reflectivity; YDF, ytterbium-doped fiber; OC, output coupling; CLS, cladding light stripper; GDF, germanium-doped fiber; QBH, quartz block head.

for cladding power and resident pump light removal, and a mode-field-matched quartz block head (QBH) is spliced after the CLS for laser output. The beam quality factors at the seed output end and main amplifier output end are both about ~1.30, which implies that both pump and signal combiner have little impact on laser beam quality.

3. Experimental Results

The fiber length and pump wavelength are set to 30 m and 976 nm, respectively, in the first experiment. The bending diameter of the fiber is about 18 cm for effective HOM suppression, and the fiber is evenly spaced on the water-cooled plate. The launched seed power is kept at ~100 W in the following experiments. In order to detect TMI, a photodiode with wavelength range of 200–1100 nm and bandwidth of 150 MHz is employed near the power meter to monitor the backscattered signal light of the main amplifier. The output properties of the constructed fiber amplifier are characterized, as shown in Fig. 4. The output power increases almost linearly and reaches 3.39 kW at the pump power of 3.86 kW, with a slope efficiency of ~84.1%. No power rollover is observed during the power scaling process. The output spectra at different output powers are depicted in Fig. 3(b), where no sign of SRS could be observed, which

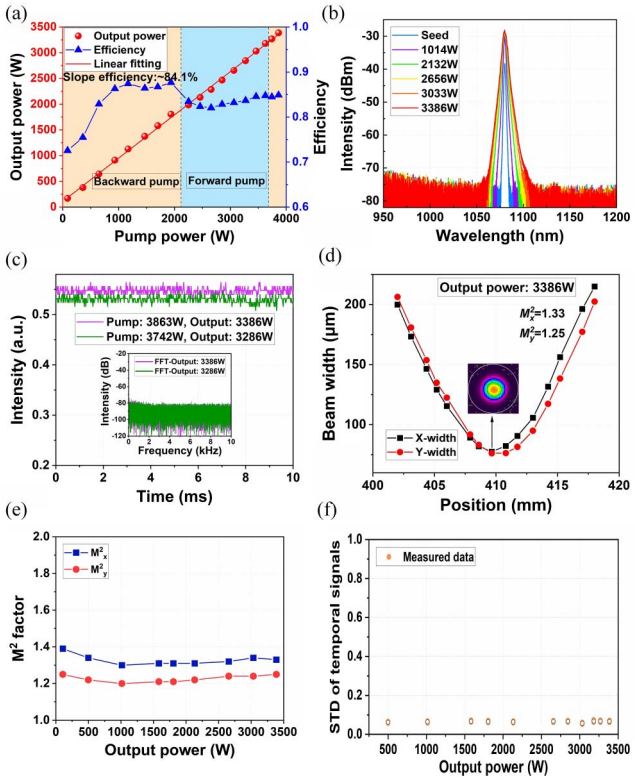

Fig. 4. (a) Output power; (b) spectrum; (c) output time/frequency domain (inset); (d) beam waist spot; (e) beam quality; (f) STD at various output powers for experiment 1.

indicates the potential for further power scaling. However, rapid fluctuation occurs in the time trace and the intensity of the low-frequency components in the frequency domain starts to increase at the output power of ~3.39 kW, as shown in Fig. 3(c). According to the criteria of the TMI phenomenon[24], when TMI occurs, the signal of the time domain suffers more severe fluctuation, and more frequency components appear on the corresponding Fourier spectra. Thus the TMI threshold is ~3.39 kW. The beam quality factor at the output power of 3.39 kW is measured to be 1.33 and 1.25 in the horizontal and vertical directions, respectively, and the beam profile remains a near-Gaussian shape, as presented in Fig. 3(d). The M^2 factor and standard deviation (STD) remain nearly constant during the power scaling process. It could be inferred that power rollover would happen as the pump power further increases owing to the stronger TMI effect. Therefore, further power scaling is limited by the TMI. On the other hand, the excellent single-mode performance can be attributed to the low-NA feature of the fiber, which leads to high bending loss for HOMs, even with a large core diameter.

A previous report has revealed that the pump wavelength could significantly affect the TMI threshold by affecting the pump absorption as well as heat generation in the fiber amplifier[25]. Generally, a high absorption coefficient at ~976 nm will cause a strong thermal gradient in the core, which directly lowers the TMI threshold even though the HOMs experience high

bending loss. In order to further improve the TMI threshold, the pump wavelength is shifted to 981 nm to deviate from the dominant 976 nm absorption peak. As a result, the maximum output power reaches 4.02 kW, with the slope efficiency of ~79.1%. The slightly lower slope efficiency compared to 976 nm pump is due to the relatively insufficient pump absorption. The output spectra at different output powers are shown in Fig. 5(b), and the signal-to-Raman ratio is ~32 dB at the maximum output power. The time trace and corresponding Fourier spectrum remain stable during the power scaling process, as presented in Fig. 5(c), which indicates the fiber amplifier is free from TMI. The beam quality factor remains around 1.30 during the entire experiment, and the output beam profile at the maximum output of 4.02 kW also maintains a Gaussian shape, as shown in Fig. 5(d). However, due to the insufficient pump absorption, an obvious temperature rise is seen on both pump combiners. For safety reasons, the pump power was not further increased.

In the third experiment, the fiber length is increased to 35 m to ensure sufficient pump absorption and suitable SRS suppression. In addition, a QBH with pigtail fiber of 30/400 μm is used to suppress the SRS effect to reduce the impact of longer YDF as much as possible. With these optimizations, the maximum output power reaches 4.96 kW at the pump power of 6.20 kW, with the corresponding optical–optical efficiency of ~78.3%, as shown in Fig. 6(a). When the output power is 4.68 kW, the signal-to-Raman ratio is ~27 dB, and when the output power is

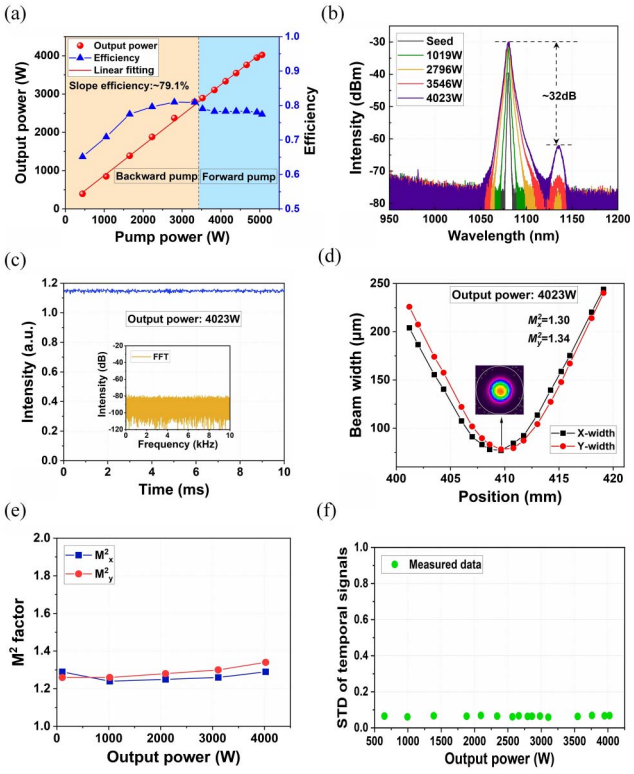

Fig. 5. (a) Output power; (b) spectrum; (c) output time/frequency domain (inset); (d) beam waist spot; (e) beam quality; (f) STD at various output powers for experiment 2.

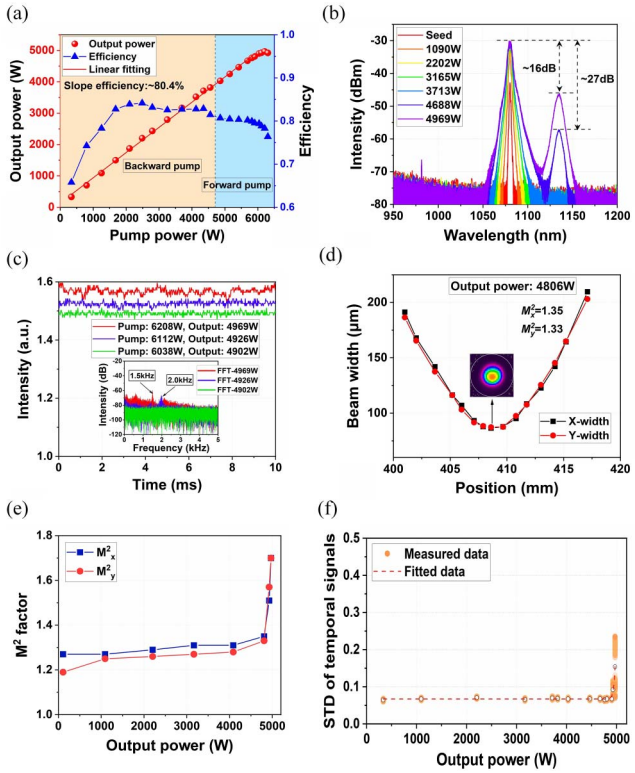

Fig. 6. (a) Output power; (b) spectrum; (c) output time/frequency domain (inset); (d) beam waist spot; (e) beam quality; (f) STD at various output powers for experiment 3.

further increased to 4.96 kW, the signal-to-Raman ratio decreases to ~16 dB. Moreover, at the power level of 4.96 kW, strong fluctuation is observed in the time trace, and multiple kilohertz characteristic frequency peaks appear on the corresponding Fourier spectrum. When the output power is 4.80 kW, the beam quality factor maintains at ~1.33. However, when the output power reaches 4.96 kW, the beam quality factor degrades to ~1.7. Combined with the degradation of the beam quality and the fluctuation of the time-frequency domain signal, it shows that the TMI effect has occurred at the output power of 4.92 kW.

The relevant key parameters of experiments 1 to 3 are summarized in Table 1.

4. Discussion

According to the previous report by Jena University[26], reduction of fiber core NA is beneficial to improve the single-mode guiding performance of the fiber, and the TMI threshold could also be significantly increased compared with the fiber with conventional NA, which has also been proven effective in this work. However, the core diameter and the NA are both slightly increased with respect to the low-NA fiber shown in Ref. [14]. On the one hand, the main obstacle for scaling the single-mode laser power for the fibers with the diameter of 20–25 μm is the nonlinear effects (especially SRS), so slightly larger diameter is beneficial for the SRS suppression under a high-power regime.

Table 1. Summary of Key Parameters of Experiments 1 to 3.

Experiment	Pump wavelength (nm)	Fiber length (m)	Bending diameter (cm)	Max output power (kW)	Limitation
1	976	30	18	3.39	TMI
2	981	30	18	4.02	Insufficient absorption
3	981	35	18	4.96	TMI, SRS

And slightly higher NA can accept a higher Yb^{3+} concentration, which will help to improve the absorption and shorten the YDF length for suppressing SRS. Note that the demonstrated NA in this Letter is lower than the conventional NA, which guarantees a high HOM suppression ability. On the other hand, the increasing of the core diameter and the NA will inevitably increase the V-value of the fiber, indicating a lower TMI threshold. To further increase the TMI threshold for higher-power scaling, a 981-nm-pumping strategy is employed here to homogenize the heat load along the fiber by reducing the quantum defect and local heat generation[27–29]. According to a previous investigation, the optimal backward pump power fraction for TMI mitigation is ~75% and ~60% for 20/400 μm and 30/400 μm fiber, respectively[30]. Finally, the TMI threshold has significantly increased from ~3.39 kW (experiment 1) to ~4.80 kW (experiment 3). In experiment 3, both TMI and SRS have occurred, where the TMI is believed to be relevant to the SRS[31]. However, 981 nm pumping suffers from the low absorption feature in experiment 2, and thus the fiber length is increased by 5 m in experiment 3, which eases insufficient pump absorption but is detrimental to the SRS suppression. Therefore, we believe that the fiber NA could be increased to ~0.050–0.052 with slightly higher Yb^{3+} concentration to ensure adequate 981 nm absorption and shorter fiber length. Also, the combination of low NA and confined doping will be explored to further increase the single-mode power scaling performance. Moreover, fiber tapering might be a possible solution to increase SRS threshold and maintain the TMI threshold; the fiber proposed in Ref. [32] is one of the potential solutions. In all, we have reported the low-NA double-clad YDF enabling the highest laser power with single-mode beam quality and all-fiber structure until now by balancing the trade-off between the nonlinear effects and TMI suppression provided by the specially designed fiber.

5. Conclusion

In this paper, LMA low-NA double-clad YDF with core/inner cladding diameter of 25/400 μm and core NA of 0.049 was designed and fabricated through MCVD in conjunction with the gas phase doping technique for high-power single-mode laser operation. Subsequently, an experimental study was carried out to investigate the impact of fiber length and pump wavelength on the power scaling potential of the self-developed low-NA fiber and the corresponding limiting factors. By shifting the pump wavelength away from the main absorption peak at 976 nm and optimizing the YDF length for sufficient pump absorption, the TMI threshold has been significantly improved. from ~3.39 kW to ~4.80 kW. As a result, the output power of 4.80 kW with near-diffraction-limited beam quality (M^2 ~ 1.33) was finally realized, which is the highest output power ever reported in low NA fiber-based fiber laser systems. This work could provide a good reference for further power scaling of single-mode fiber laser utilizing the LMA specialty optical fiber.

Acknowledgements

This work was supported by the National Key R&D Program of China (No. 2022YFB3606000) and State Key Laboratory of Pulsed Power Laser Technology (No. SKL2021ZR06).

References

1. V. Gapontsev, V. Fomin, A. Ferin, *et al.*, "Diffraction limited ultra-high-power fiber lasers," in *Lasers Sources and Related Photonic Devices* (2010), paper AWA1.
2. J. Hecht, "High-power fiber lasers," Opt. Photonics News **29**, 30 (2018).
3. C. Jauregui, J. Limpert, and A. Tünnermann, "High-power fibre lasers," Nat. Photonics **7**, 861 (2013).
4. X. Chen, T. Yao, L. Huang, *et al.*, "Functional fibers and functional fiber-based components for high-power lasers," Adv. Fiber Mater. **5**, 59 (2023).
5. R. Paschotta, J. Nilsson, P. R. Barber, *et al.*, "Lifetime quenching in Yb-doped fibres," Opt. Commun. **136**, 375 (1997).
6. S. Taccheo, H. Gebavi, A. Monteville, *et al.*, "Concentration dependence and self-similarity of photodarkening losses induced in Yb-doped fibers by comparable excitation," Opt. Express **19**, 19340 (2011).
7. H.-J. Otto, N. Modsching, C. Jauregui, *et al.*, "Impact of photodarkening on the mode instability threshold," Opt. Express **23**, 15265 (2015).
8. C. Jauregui, H.-J. Otto, F. Stutzki, *et al.*, "Simplified modelling the mode instability threshold of high power fiber amplifiers in the presence of photodarkening," Opt. Express **23**, 20203 (2015).
9. R. Tao, P. Ma, X. Wang, *et al.*, "Influence of core NA on thermal-induced mode instabilities in high power fiber amplifiers," Laser Phys. Lett. **12**, 085101 (2015).
10. M. Li, X. Chen, A. Liu, *et al.*, "Limit of effective area for single-mode operation in step-index large mode area laser fibers," J. Light. Technol. **27**, 3010 (2009).
11. Y. Jeong, J. K. Sahu, D. N. Payne, *et al.*, "Ytterbium-doped large-core fiber laser with 1.36 kW continuous-wave output power," Opt. Express **12**, 6088 (2004).
12. V. Khitrov, J. D. Minelly, R. Tumminelli, *et al.*, "3 kW single-mode direct diode-pumped fiber laser," Proc. SPIE **8961**, 89610V (2014).
13. D. Jain, Y. Jung, P. Barua, *et al.*, "Demonstration of ultra-low NA rare-earth doped step index fiber for applications in high power fiber lasers," Opt. Express **23**, 7407 (2015).
14. L. Huang, T. Yao, J. Leng, *et al.*, "Mode instability dynamics in high-power low-numerical-aperture step-index fiber amplifier," Appl. Opt. **56**, 5412 (2017).

15. F. Beier, C. Hupel, J. Nold, *et al.*, "Narrow linewidth, single mode 3 kW average power from a directly diode pumped ytterbium-doped low NA fiber amplifier," Opt. Express **24**, 6011 (2016).
16. F. Beier, C. Hupel, S. Kuhn, *et al.*, "Single mode 4.3 kW output power from a diode-pumped Yb-doped fiber amplifier," Opt. Express **25**, 14892 (2017).
17. F. Beier, F. Möller, B. Sattler, *et al.*, "Experimental investigations on the TMI thresholds of low-NA Yb-doped single-mode fibers," Opt. Lett. **43**, 1291 (2018).
18. Y. Midilli and B. Ortaç, "Demonstration of an all-fiber ultra-low numerical aperture ytterbium-doped large mode area fiber in a master oscillator power amplifier configuration above 1 kW power level," J. Light. Technol. **38**, 1915 (2020).
19. F. Zhang, Y. Xing, L. Liao, *et al.*, "Thermo-optic behaviour of intrinsically single-mode low-numerical aperture (NA) ytterbium-doped fibre," Laser Phys. **29**, 075106 (2019).
20. R. Liu, D. Yan, Z. Fan, *et al.*, "Fabrication and 1046 nm laser behaviors of Yb-doped phosphosilicate binary fiber with a pedestal structure," Opt. Mater. Express **10**, 464 (2020).
21. D. J. DiGiovanni, "Fabrication of rare-earth-doped optical fiber," Proc. SPIE **1373**, 2 (1991).
22. E. H. Sekiya, P. Barua, K. Saito, *et al.*, "Fabrication of Yb-doped silica glass through the modification of MCVD process," J. Non-Cryst. Solids **354**, 4737 (2008).
23. D. Marcuse, "Curvature loss formula for optical fibers," J. Opt. Soc. Am. **66**, 216 (1976).
24. H. J. Otto, F. Stutzki, F. Jansen, *et al.*, "Temporal dynamics of mode instabilities in high-power fiber lasers and amplifiers," Opt. Express **20**, 15710 (2012).
25. K. Hejaz, A. Norouzey, R. Poozesh, *et al.*, "Controlling mode instability in a 500 W ytterbium-doped fiber laser," Laser Phys. **24**, 025102 (2014).
26. N. Haarlammert, B. Sattler, A. Liem, *et al.*, "Investigations of mode instabilities in low-NA reduced mode overlap photonic crystal fibers," in *European Conference on Lasers and Electro-Optics - European Quantum Electronics Conference* (2015), paper CJ_10_3.
27. Y. Wan, X. Xi, B. Yang, *et al.*, "Enhancement of TMI threshold in Yb-doped fiber laser by optimizing pump wavelength," IEEE Photon. Technol. Lett. **33**, 656 (2021).
28. B. Yang, P. Wang, H. Zhang, *et al.*, "6 kW single mode monolithic fiber laser enabled by effective mitigation of the transverse mode instability," Opt. Express **29**, 26366 (2021).
29. R. Tao, P. Ma, X. Wang, *et al.*, "Mitigating of modal instabilities in linearly-polarized fiber amplifiers by shifting pump wavelength," J. Opt. **17**, 45504 (2015).
30. R. Tao, P. Ma, X. Wang, *et al.*, "Theoretical study of pump power distribution on modal instabilities in high power fiber amplifiers," Laser Phys. Lett. **14**, 025002 (2017).
31. K. Hejaz, M. Shayganmanesh, R. Rezaei-Nasirabad, *et al.*, "Modal instability induced by stimulated Raman scattering in high-power Yb-doped fiber amplifiers," Opt. Lett. **42**, 5274 (2017).
32. R. Sidharthan, D. Lin, K. J. Lim, *et al.*, "Ultra-low NA step-index large mode area Yb-doped fiber with a germanium doped cladding for high power pulse amplification," Opt. Lett. **45**, 3828 (2020).